Mine Water and the Environment (2005) 24: 186–193 © IMWA Springer-Verlag 2005

Technical Article

Use of a Multiple Orifice Spray Reactor to Accelerate Ferrous Iron Oxidation in Acidic Mine Water

Daniel B. Klein and Ronald D. Neufeld

Dept of Civil and Environmental Engineering, Univ of Pittsburgh, 949 Benedum Hall, 3700 O'Hara St, Pittsburgh, PA, USA 15261; corresponding author's e-mail: neufeld@engr.pitt.edu

Abstract. The potential of a multiple orifice spray reactor to enhance aeration and oxidation of ferrous iron in acidic mine water was investigated in a bench-scale experiment. The reactor consists of two concentric cylinders, with a series of orifices that act like a venturi in the inner cylinder. Neutralization and aeration are combined in the reaction chamber where air is aspirated and alkaline agent dispensed. Ferrous iron oxidation rates were about four orders of magnitude faster than theoretical rates at a treatment pH of 6.5; at an influent ferrous iron concentration of around 150 mg/L, the orifice spray reactor oxidized about 30% of the ferrous to ferric iron within 1 second. Under certain conditions, the orifice spray reactor oxidizes more ferrous iron than can be simply attributed to the oxygen transfer capabilities of the system. It is suggested that the excess oxidation capability is due to, or initiated by, the effects of hydrodynamic cavitation.

Key words: Acid mine drainage; aeration; cavitation; hydrodynamic cavitation; iron; mine drainage; orifice; orifice spray reactor; oxidation; oxygen transfer

Introduction

Acid mine drainage (AMD) is an international problem. Many mine discharges are neutralized by the addition of an alkaline agent and mechanically aerated to oxidize dissolved metals, especially iron. The rate of iron oxidation increases 10-fold with each unit increase in pH. Often, this oxidation reaction defines how much alkalinity must be used.

A multiple orifice spray reactor (MOSR) is an alternative active treatment device that requires a small "footprint" of land space, and can oxidize iron rapidly (Smith and Werner 1984). A commercial MOSR device has been marketed under the trade name, Turbojett®. Kolbash and Budeit (1988) reported the field scale use of an early Turbojett® prototype, which was retrofitted into an existing AMD treatment system at a mine in Ohio. They reported that effluent iron limits were never exceeded when that technology was employed, and that iron oxidation was accelerated, but did not report actual rates. This paper presents data and information regarding enhanced ferrous iron oxidation based on experiments conducted with a bench-scale MOSR.

Background

Ferrous iron oxidizes to the ferric form according to:

$$Fe^{+2} + \tfrac{1}{4}\, O_2 + H^+ \rightarrow Fe^{+3} + \tfrac{1}{2}\, H_2O \qquad (1)$$

Stumm and Lee (1961) have previously reported the kinetics of ferrous iron oxidation to be:

$$-d[Fe^{2+}]/dt = k[OH^-]^2 P_{O2}[Fe^{2+}] \qquad (2)$$

where k is the rate constant ($M^{-2}atm^{-1}min^{-1}$), $[OH^-]$ is the hydroxyl ion concentration, and $[Fe^{2+}]$ is the total ferrous iron concentration. Another Fe^{2+} oxidation rate law was developed by the U.S. Bureau of Mines (USBM), based on laboratory and field tests using an "In–Line System" (ILS), an active single orifice system incorporating a pump, a venturi, and a static mixer (Ackman and Kleinmann 1984). This simple system showed enhanced Fe^{+2} oxidation rates and reduced residence time and land requirements Venturi devices involve flow through a pipe with a sharply decreasing and then increasing diameter; the reduced pressure can be used to aspirate air or other fluids into the venturi throat. When using the ILS system, at iron concentrations higher than those used by Stumm and Lee, Fe^{+2} oxidation rates were much greater than would be predicted using equation 1. The USBM developed an oxygen dependent, Fe^{2+} oxidation model, which was validated experimentally using the ILS for very high Fe^{+2} concentrations. The USBM model is based on the assumption that oxygen transfer is the rate limiting step. This model takes into account the O_2 transfer rate and the stoichiometric constant relating iron and O_2 in the oxidation reaction. The basic relationship is:

$$\frac{d[O_2]}{dt} = ko_2([O_2]_{sat} - [O_2]_t) \qquad (3)$$

where k_{O2} = O_2 mass transfer coefficient, minutes^{-1}; $[O_2]_{sat}$ = O_2 at saturation, mg/L; and $[O_2]_t$ = time dependent concentration of O_2, mg/L. Assuming that O_2 transfer is the rate limiting step, the rate of Fe^{2+} oxidation can be written as (Ackman et al. 1984):

$$\frac{-d[Fe^{2+}]}{dt} = \frac{7d[O_2]}{dt} = 7kO_2([O_2]_{sat} - [O_2]_t) \quad (4)$$

where $[Fe^{2+}]$ = Fe^{2+} concentration in mg/L. The factor of 7 comes from the stoichiometric relationship displayed in equation (1). This relationship shows that 55.85 mg/L of Fe^{2+} is oxidized by 8 mg/L of O_2.

As previously stated, during Fe^{2+} oxidation, O_2 is rapidly consumed and $[O_2]_t << [O_2]_{sat}$ and equation (4) becomes:

$$\frac{-d[Fe^{2+}]}{dt} = 7kO_2[O_2]_{sat} \quad (5)$$

It was initially reported that the amount of Fe^{2+} oxidized by the ILS was always greater than the stoichiometric amount of iron that could be oxidized based on the measured oxygen transfer capabilities of the system. Ackman and Kleinmann (1984) opined that the ILS was either catalyzing the rate of reaction (creating micro-environments at high pH) or somehow creating a catalyst. However, Hustwit et al. (1992) subsequently attributed this observation to experimental error.

Materials and Methods

Multiple Orifice Spray Reactor (MOSR)

A MOSR is physically comprised of two concentric cylinders (Figure 1). Figure 2 shows the experimental set up of a bench-scale MOSR within the University of Pittsburgh's environmental engineering laboratory. The maximum flow rate to the bench scale MOSR unit was limited by pump capacity to 1 gpm (3.78 L/min). The height of the inner cylinder (reaction chamber) is 3.5 inches (8.9 cm) and the annulus is 0.25 inches (0.56 cm). The inside cylinder has two rings containing 12 orifices with diameter 0.018 inch (0.05 cm) (Figure 1). These orifices are 9/16 inch (1.4 cm) in length.

AMD was collected from St. Michael's mine, Cambria County Pennsylvania; its composition is shown on Table 1. The St. Michael's mine discharge flows into Topper Run tributary at a flow rate of 2,000 – 4,000 gpm (5,400 – 10,800 L/min.). St. Michael's AMD was transported to the laboratory in plastic containers sealed from atmospheric intrusion. AMD used for any given experimental run was placed into a sealed

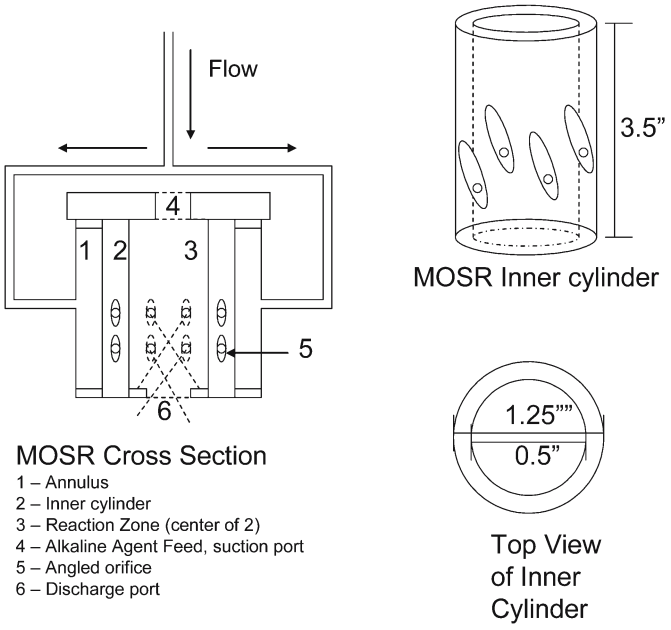

Figure 1. Experimental MOSR schematic

Table 1. St. Michael's Mine water quality

Selected Mining Constituents	Topper Run, St. Michael's Mine
pH	3.1
Sulfate	1100 mg/L as SO_4
Iron	174 mg/L
Manganese	4.9 mg/L
Aluminum	0.58 mg/L

reservoir (Figure 2). Nitrogen was continuously bubbled through the reservoir to assure minimal if not zero levels of dissolved oxygen in the AMD sample. AMD was then pumped from the reservoir (using a SHURFLO industrial transfer diaphragm pump) to the MOSR. As shown in Figure 2, an in-line flow meter, sampling valves, a pressure gauge, and valves for controlling flow and pressure to the reaction chamber are incorporated in the experimental system.

The water enters the MOSR through two oppositely sited inlet ports (Figure 1) into a chamber that consists of an annulus of two cylinders (area 1, Figure 1). The inside cylinder is hollow, open at both ends, and has a number of engineered orifices (area 5, Figure 1) arranged so that liquid forced through the orifices is discharged with vector components that promote a helical pattern (area 6, Figure 1) as well as a component directed towards the cylinder's discharge end.

Due to the relatively small diameter of these orifices, the maximum pressure on the inlet side of the orifices can be maintained at a maximum of 100 psi (689 KPa), with the actual operating pressure being controlled by the inlet flow rate. The entire measured pressure drop through the experimental system was found to be the

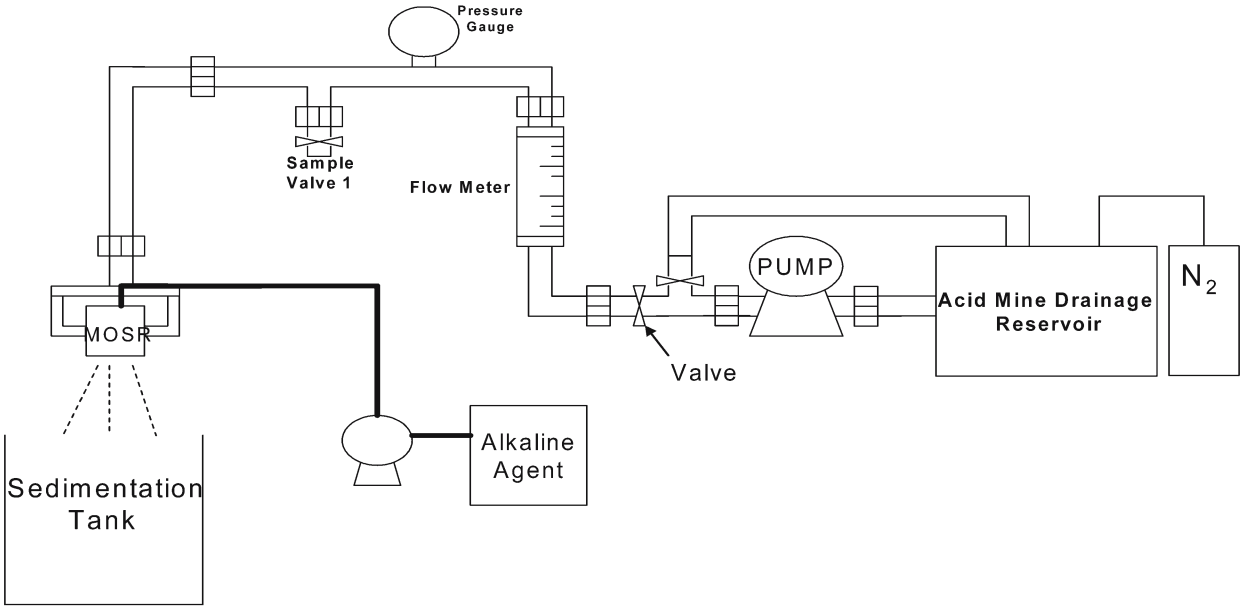

Figure 2. Experimental Setup

result of flow through the orifices; the pressure drop through the valves, pipe, flow bends and flow meters were negligible. To demonstrate this, an experiment was conducted with the inner cylinder (area 2, Figure 1) removed from the system. Water was pumped through the system at approximately 1.0 gpm (2.7 L/min) with virtually no pressure drop caused by the piping system or geometrical configuration of the MOSR casing.

The MOSR creates a discharge spray that can be directed into a sampling container or sedimentation tank that is open to the atmosphere (Figure 2). The venturi action creates a pressure differential, and air is drawn into the center of the inner cylinder where aeration and oxidation takes place (areas 3 and 4, Figure 1). Supplemental alkaline agents are introduced into the inner cylinder in calibrated quantities, as appropriate. For all of these experiments, an aqueous solution of 0.1 N NaOH was introduced into the gas suction end of the MOSR with a calibrated peristaltic pump. The flow rate was determined by the desired end-point pH, accounting for the anticipated stoichiometric oxidation and Fe^{2+} hydrolysis, in which 2 mols of H^+ are produced for every mol of Fe^{2+} oxidized.

The residence time used in calculating the gas transfer rates was based on the space time of the reactor. The experiments for this purpose were carried out at an operating flow of 0.7 gpm (2.6 L/min), a pressure of approximately 75 psi (517 KPa), and 20° C, unless otherwise noted. The residence time (RT) of liquid in the reaction zone (the inside of the center cylinder) was computed as:

RT = volume/flow rate = 45.06 cm^3/2649.79 cm^3/min = 0.017 min = 1.02 sec.

Oxygen Transfer Coefficients

The oxygen transfer coefficient was determined as Hustwit et al. (1992) did, starting with the basic relationship of oxygen transfer into water:

$$\frac{d[O_2]}{dt} = ko_2([O_2]_{sat} - [O_2]_t) \qquad (6)$$

where ko_2 = the oxygen transfer coefficient, sec^{-1}, $[O_2]_{sat}$ = the oxygen concentration at saturation, mg/L, $[O_2]_t$ = the oxygen concentration at time t, mg/L, and $[O_2]$ = oxygen concentration, mg/L.

A known volume of tap water was initially deoxygenated using sodium sulfite and pumped through the MOSR. Samples were taken immediately before and after the reactor (sample valve 1, Figure 2). Re-entrainment of O_2 was minimized by fixing a funnel directly beneath the discharge of the MOSR while holding the water level in the top of the funnel constant at the outlet of the MOSR with the water jets exiting the MOSR being submerged. Oxygen was measured using an Orion dissolved oxygen probe attached to a pH meter. The value of O_2 transferred in the residence time within the chamber resulted in a calculated oxygen transfer rate ($d[O_2]/dt$).

Ferrous Iron Oxidation Measurements

The MOSR Fe^{2+} oxidation rate was compared to equation 2 using a rate constant (k) of 3.0E-12 $minute^{-1}mol^{-1}$ (Hustwit et al. 1992) at 20°C. The Fe^{2+}

oxidation rate using the MOSR was not compared to the USBM model, which was only validated for initial Fe^{2+} concentrations greater than 800 mg/L. Ackman et al. (1984) reported that the USBM model was tested using the ILS at an initial Fe^{2+} concentration of 300 mg/L and in that case, the iron dependent model (equation 2) did indeed apply. The experimental Fe^{2+} oxidation rates were computed by measuring the change in Fe^{2+} concentrations between the influent and effluent of the MOSR. This change in Fe^{2+} concentration was then divided by the hydraulic residence time to determine Fe^{2+} oxidation rates.

In addition to AMD, laboratory control samples were prepared using reagent grade ferrous sulfate ($FeSO_4 \cdot 7H_2O$) in deionized water. All samples were sealed with a nitrogen blanket as described above to minimize Fe^{2+} to Fe^{3+} conversion in the feed tank. The dissolved oxygen (DO) levels in the AMD feed reservoir were kept between 0 and 1.0 mg/L using a constant nitrogen purge, and was monitored with a DO meter during the course of the experiment.

Aqueous samples were taken and analyzed for Fe^{2+} concentrations prior to entering the MOSR (sample valve 1, Figure 2) and upon leaving the MOSR. Ferrous iron was determined using the Fe B-phenanthroline method (procedure #3500, APHA et al. 1998). Sampling containers were prepared with 2 mL of concentrated HCL per 100 mL of sample to limit further iron oxidation prior to analysis.

Results and Discussion

Oxygen Transfer Capabilities

A series of four replicate tests were completed at a flow rate of 0.7 gpm (1.9 L/min) and 70 psi (483 KPa) to determine the oxygen transfer coefficient, K_{O2}. At 23.2°C, K_{O2} was determined to be 28.1 min^{-1}. The value of k_{O2} at 20°C was approximated as 26.04 min^{-1} using a form of the van't Hoff–Arrhenius relationship, $K_La_{(T)} = K_La_{(23.2°C)}\Theta^{T-23.2}$ with the selected value of Θ = 1.024, a value typical for mechanical aerators (Metcalf & Eddy 2003). For comparison purposes, the ILS system had a K_{O2} value of 9.07 min^{-1} (Ackman and Kleinmann 1984). The laboratory tests conducted using the ILS were carried out at flow rate of 10 gpm (37.8 L/min) and a pressure ranging from 20 – 50 psi (138 – 345 KPa). Tests conducted on the MOSR (Klein 2005) showed K_{O2} value of 18 min^{-1} at 20 psi (138 KPa), 23.5°C, and 0.3 gpm (1.1 Lpm). This comparison suggests the MOSR exhibits about three times the gas transfer coefficient of the ILS system, reflecting the different geometrical configuration; the k_{O2} value representative of a venturi like system is likely a function of the number of orifices and the pressure drop and hence the geometry of the system. The MOSR has multiple orifices whereas the ILS only has one. It should be noted that the MOSR used in this work is a laboratory prototype system; larger scaled systems with refinements in reactor geometry might further enhance the oxygen transfer coefficient and chemical oxidation capabilities.

In order to demonstrate that all the mass transfer was taking place in the reaction zone of the MOSR, an experiment was conducted where the suction port (area 4, Figure 2) was sealed with a stopper, preventing inlet air flow. The water was deoxygenated as previously described and any changes in oxygen were measured across the MOSR. The measured oxygen transfer across the system was about 0.9 mg/L DO, which may reflect oxygen transfer during laboratory manipulation of the samples; regardless, the mass transfer of oxygen was shown to largely take place in the reaction zone.

Equation 1 suggests that for every 1 mg of oxygen used, approximately 7 mg Fe^{2+}/L is oxidized. The laboratory MOSR unit transfers 4.16 mg/L of oxygen when the inlet DO is 0.5 ± 0.5 mg/L. Based on the stoichiometry and oxygen transfer abilities, the MOSR should theoretically be able to oxidize approximately 30 mg/L of Fe^{+2} in one pass through at normal temperature and pressure.

Ferrous Iron Oxidation

The actual MOSR Fe^{+2} oxidation rates were measured as a function of pH and compared to literature values. This was accomplished by the introduction of calibrated levels of liquid sodium hydroxide into the suction side of the MOSR and maintenance of final pH values at the immediate outlet of the MOSR.

Samples were collected in containers prepared with acid to prevent further Fe^{+2} oxidation in the sampling container. Figure 3 compares measured Fe^{+2} rates with data from the Stumm model (Stumm and Lee 1961). This figure shows that the lab scale MOSR exhibits a Fe^{+2} oxidation rate 3.5 or more orders of magnitude greater than that which would be predicted at a final pH value of 6.5 or less. The relative kinetic advantage diminishes as the effluent pH approaches 8.0.

Since the sodium hydroxide is injected directly into the throat of the MOSR, the hypothesis suggested by Ackman and Kleinmann (1984) for the ILS, of a localized microenvironment with elevated pH values appears reasonable. It is likely that the Fe^{+2} rapidly precipitates as $Fe(OH)_2$ in this zone. It is well known that hydroxo complexes of metal ions are oxidized faster by O_2 than simple aqueous metal ions (Stumm

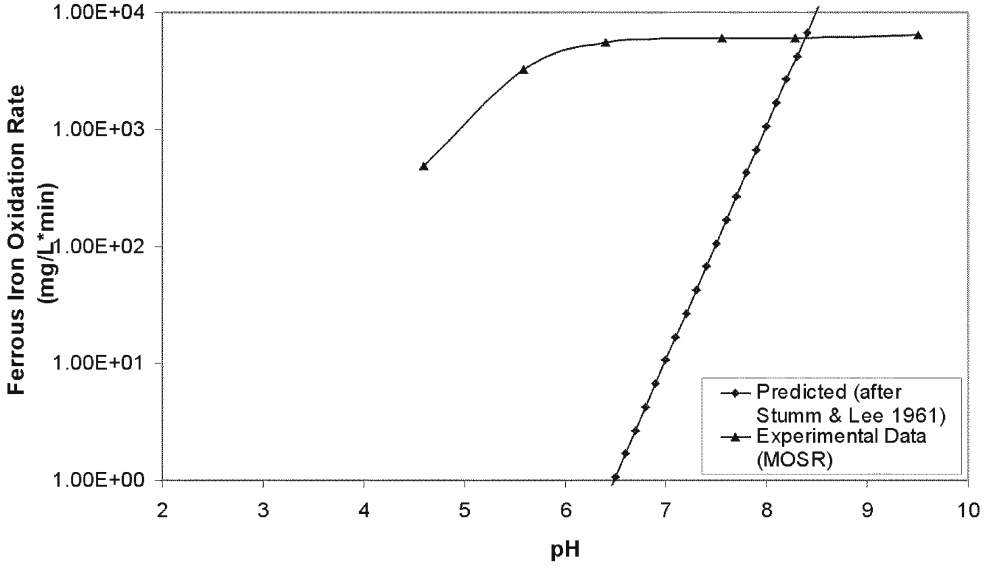

Figure 3. Experimental MOSR and predicted oxidation rates

and Morgan 1996). In addition, some gas phase reactions would be taking place in the zone of cavitation. Gas phase diffusion coefficients are greater by several orders of magnitude than liquid phase coefficients. Both explanations, when taken together, may explain why ferrous iron is rapidly converted to ferric ion within the short detention time of the MOSR. A material balance conducted around the reaction zone of the MOSR indicated that the pH reaches a value of 11 in the reaction zone, assuming that all reactions were in the aqueous phase. This high pH then falls to 7 or less in the sedimentation tank by the production of hydrogen ions during iron hydrolysis reactions.

A series of experiments were conducted on the control Fe^{+2} water samples and the St. Michaels AMD water samples, as outlined above. The Fe^{+2} control solutions in the AMD reservoir was kept deoxygenated with nitrogen gas, and had an initial pH between 6.0 and 7.5. In each test, a calibrated flow of 0.1 M NaOH was maintained and the ferrous-rich AMD or control solution feed flow rate were 0.78 gpm (2.7 L/min) through the MOSR. Table 2 is a summary of the experimental data and shows that the quantity of ferrous iron oxidized was greater than could be explained by oxygen transfer alone. The excess was calculated according to equation 7:

$$\frac{\Delta Fe^{+2}{}_{EOC}}{\Delta t} = \frac{\Delta Fe^{+2}{}_{MOSR}}{\Delta t} - \frac{\Delta Fe^{+2}{}_{OT}}{\Delta t} \qquad (7)$$

where $\Delta Fe^{+2}{}_{EOC}$ = Fe^{+2} oxidized due to an excess oxidant contribution (mg/L), $\Delta Fe^{+2}{}_{MOSR}$ = measured ferrous iron change across the MOSR (mg/L), and $\Delta Fe^{+2}{}_{OT}$ = ferrous iron oxidized due to the measured oxygen transfer capability of the MOSR (mg/L).

Deoxygenating with nitrogen gas in the experimental system could not consistently produce an AMD feed

Table 2. Results of ferrous oxidation test; all tests were conducted at 70 psi ±10psi; all concentrations are in mg/L

Sample	Initial pH	Final pH	Initial DO	Initial Fe^{+2}	Final Fe^{+2}	$\Delta Fe^{+2}{}_{MOSR}$	$\Delta Fe^{+2}{}_{OT}$	Stoichiometric amount of Fe^{+2} that can be oxidized by the DO in the system	$\Delta Fe^{+2}{}_{EOC}$ (mg/L Fe^{+2})	$\Delta Fe^{+2}{}_{EC}$ (mg/l O_2)
1.AMD	6.60	9.00	0.66	137.51	77.98	59.52	5.16	36.12	23.40	3.34
2.AMD	6.65	9.40	0.70	139.95	86.14	53.82	5.20	36.40	17.42	2.49
3.AMD	6.00	8.28	0.70	141.59	82.47	59.12	5.20	36.40	22.72	3.25
4.AMD	6.65	9.30	0.70	141.59	81.25	60.34	5.20	36.40	23.94	3.42
5.AMD	6.00	8.24	0.66	142.40	88.58	53.82	5.16	36.12	17.70	2.53
6.AMD	6.20	8.80	0.58	143.22	90.22	53.00	5.08	35.56	17.44	2.49
7.AMD	7.50	7.30	0.80	152.59	102.85	49.74	5.30	37.10	12.64	1.81
8.Control	6.50	7.00	0.80	200.29	152.59	47.70	5.30	37.10	10.60	1.51
9.Control	7.50	7.30	0.80	200.29	144.03	56.26	5.30	37.10	19.16	2.74
10.Control	6.70	6.80	0.90	303.56	256.10	47.46	5.40	37.80	9.66	1.38

$\Delta Fe^{+2}{}_{MOSR}$ = measured ferrous iron change across the MOSR; $\Delta Fe^{+2}{}_{OT}$ = ferrous iron oxidized due to measured oxygen transfer capabilities of the MOSR; $\Delta Fe^{+2}{}_{EOC}$ = ferrous iron oxidized due to an excess oxidant contribution

water with a DO reading of 0 mg/L. In order to correct for the oxygen present in the feed water, the quantity of $\Delta Fe^{+2}{}_{OT}$ (ferrous ion conversion equivalent due to the inlet dissolved oxygen) was adjusted upwards to correct for the DO level measured in the feed water. The variability in the amount of O_2 transferred was on the order of 10%.

For conservative calculation purposes, the $\Delta Fe^{+2}{}_{OT}$ value used was the average amount of O_2 transferred plus the standard deviation. This provided a value for calculation purposes of 4.5 mg/L of DO being transferred. The last column of Table 2, titled $\Delta Fe^{+2}{}_{EOC}$ (mg/L O_2), shows the apparent formation of excess oxidizing ability. The laboratory MOSR displayed an excess oxidizing ability of 2.5 mg/L of oxygen equivalent at a minimum, or an excess oxidizing ability of about 1.55 times that due to aeration alone [(4.5+2.5)/4.5].

Cavitation and Free Radicals

It is known that when flow enters a sharp edged orifice, the flow detaches from the sides of the orifice and forms a vena contracta. The contraction at a venturi inlet sufficiently reduces the cross sectional area of the flow for this to occur. This reduced flow area results in a localized increase in liquid velocity and a subsequent pressure drop. If the absolute pressure falls below the vapor pressure of the liquid, then cavitation results, with vapor cavities forming within the bulk fluid. Tseng and Collicott (2000) report that cavitation in an orifice is almost always present in flow through an orifice at and downstream of the inlet hole, and has been demonstrated from 4 psi to 30,458 psi (30 KPa to 210 MPa). As the pressure in the bulk liquid recovers, these cavities rapidly collapse. In the case of the MOSR, the recovered pressure (outlet) is approximately equal to atmospheric.

One way to assess the occurrence of cavitation in fluid flow through an orifice is through the use of Bernoulli's equation. From Bernoulli's equation, a dimensionless cavitation number, σ, can be derived which measures the resistance of flow to cavitation. The cavitation number, σ, is deduced from the relation between static pressure, P, and flow velocity, u. Bernoulli's equation states that pressure drops due to flow are proportional to the product of fluid density and the square root of the flow velocity. The cavitation number σ is obtained by dividing the available static pressure, $P_0 - P_v$, by the dynamic flow pressure (Shah et al. 1999):

$$\sigma = \frac{P_0 - P_v}{\frac{1}{2}\rho u^2} \quad (7)$$

where P_0 is the ambient pressure or pressure downstream of the orifice, P_v is the vapor pressure of the fluid flowing through the orifice, ρ is the liquid density, and u is the liquid velocity through the orifice. The particular value at which cavitation is incipient is termed the "cavitation inception number". Under ideal conditions, cavitation usually occurs for $\sigma < 1$, although cavitation inception can occur at cavitation number values greater than 1. Factors affecting cavitation inception are the geometry of the orifice and the presence of dissolved species and gases. Dissolved species, including dissolved gases, produce weak spots in the fluid continuum for cavities to form, thus enhancing cavitation (Gogate et al. 2000). When cavities collapse, localities of high temperature and pressure exist. This can enhance chemical oxidation reactions. In addition, the generation of local high temperatures and pressures induces the cleavage of water molecules and results in the formation of free radicals such as OH*, which have very strong oxidizing capabilities. Cavitation conditions can produce OH* and peroxides in accord with the following equations:

$$HOH + \text{cavitation} \rightarrow H^* + OH^* \quad (8)$$

$$H^* + O_2 \rightarrow HO_2^* \quad (9)$$

$$HO_2^* + HO_2^* \rightarrow H_2O_2 + O_2 \quad (10)$$

$$OH^* + OH^* \rightarrow H_2O_2 \quad (11)$$

Cavitation-generated oxidation was reported by Kumar et al. (2000), who used flow through an orifice plate to induce bacterial oxidation and inactivation. Kumar et al. (2000) and Suslick et al. (1997) have also shown that hydrodynamic cavitation can be used to rapidly oxidize potassium iodide to iodine. The observation of enhanced iron oxidation by Ackman and Kleinmann (1984) could also have been due to oxidants being produced by cavitation, which can take place inside a venturi as well as in an orifice.

The cavitation number for the MOSR system can be calculated based on operating conditions and the physical geometry. Ferrous iron oxidation tests were conducted at a flow rate of 0.7 gpm (2.7 L/min), pressure drop of 70 psi (101 KPa), and a liquid temperature of 25°C ±2°C. The input parameters for the cavitation number are the downstream pressure, P_0, the vapor pressure of the fluid, P_v, the density of the fluid, ρ, and the velocity of liquid through the

orifice, u. We assumed that the elevation difference between the flow upstream of the orifice and the flow in the orifices was negligible and the flow through one orifice in the MOSR was the total flow divided by the number of orifices. The density of the AMD was taken to be that of water (1000 kg/m^3) and the vapor pressure used in the calculation was the vapor pressure of water at 25°C (2.34 KPa). The ambient pressure was taken to be 1 atm (101 KPa). With these values, the cavitation number for the MOSR was calculated using equation 7:

$$\sigma = \frac{P_0 - P_v}{\frac{1}{2}\rho u^2} = \frac{101325\text{Pa} - 2339\text{Pa}}{\frac{1}{2}(1000\text{kg/m}^3)(23\text{m/s})^2} = 0.38$$

The cavitation number calculated for the MOSR is much less than unity. According to Shah et al. (1999), a cavitation number less than unity strongly suggests the occurrence of cavitation.

Effect of Initial Ferrous Iron Concentration on Ferrous Oxidation

A set of experiments was carried out to test the influence of initial inlet Fe^{+2} concentration on the measured degree of Fe^{+2} oxidation through the MOSR. The purpose of this experimental series was to quantify the maximum Fe^{+2} conversion that could be produced by the MOSR when operating at the experimental maximum flow rate. It should be noted that the results are an artifact of the inherent limitations of the laboratory setup, and field-sized systems with larger pumping and greater pressure capacities should produce results superior to that found in the laboratory.

Six different initial Fe^{+2} concentrations were tested, ranging from 50 – 1500 mg/L. The NaOH concentration (0.1 M) and flow rate (150 mL/min) were kept constant throughout the experiments. The inlet water pressure of the MOSR was kept at 75 psi (517 KPa) and the flow rate was 0.7 gpm (1.9 L/min). Deoxygenating was accomplished with N_2 sparging in the feed tank, which was maintained throughout the entire experiment. The temperature was 25°C ± 3° for all trials.

Figure 4 shows that the extent of Fe^{+2} oxidation in the MOSR is dependent on the influent Fe^{+2} concentration, with conversions approaching a maximum but constant value as the inlet Fe^{+2} concentration increases. The solid horizontal line in Figure 4 represents the calculated conversion of Fe^{+2} that can be associated with the oxygen transfer capabilities of the bench-scale MOSR. With initial Fe^{+2} concentrations equal to or above 75 mg/L, the measured mass of Fe^{+2} oxidized to the ferric state was greater than what can be attributed to the oxygen transfer capabilities of the system alone. Furthermore, the maximum conversion of Fe^{+2} approaches an upper limit, which presumably reflects the finite capability of the bench-scale MOSR to produce free oxidizing radicals at the given flow rate and pressure drop.

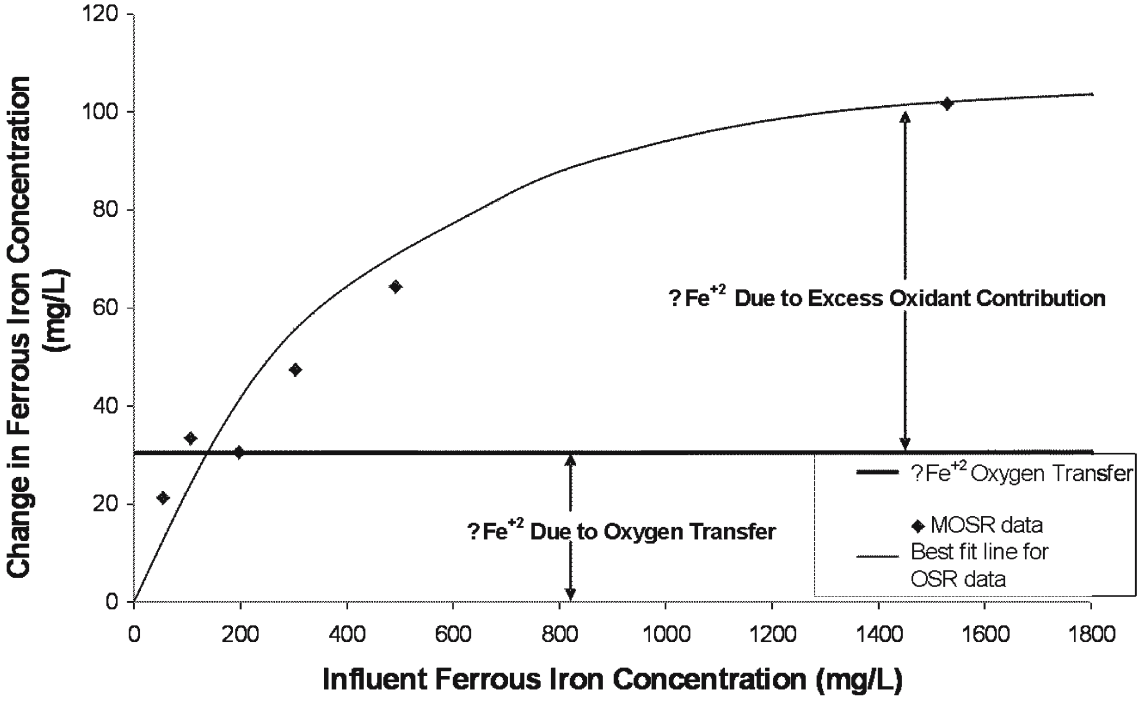

Figure 4. Ferric iron produced as a function of initial ferrous iron concentration; the solid line represents the amount of ferric iron produced by the oxygen transfer capabilities of the system. Temperature = 24±2°C

Summary and Conclusions

The multiple orifice spray reactor (MOSR), consisting of multiple orifices within an annulus, is an effective approach for the treatment of mine drainage containing Fe^{+2}, and has a rate advantage when theeffluent pH value is less than 8.0. The MOSR greatly increased Fe^{+2} oxidation rates above theoretical limits by relatively high mass transfer rates of oxygen, presumably enhancing oxidation in each of the multiple venturi throats. At an effluent pH of 6.5, the MOSR oxidizes Fe^{+2} to ferric iron at a rate about four orders of magnitude higher than theoretically predicted. These accelerated oxidation rates are likely due to cavitation and vaporization of ferrous ions within the multiple throats of the orifice reactor. In addition, it is suggested that formation of $Fe(OH)_2$ in the reactor may also contribute to increased Fe^{+2} oxidation rates.

When treating discharges with Fe^{+2} concentrations greater than 75 mg/L, the measured oxidation equivalents produced in the bench reactor are, on average, 2.5 mg of oxygen equivalent greater than can be attributed to the 4.5 mg/L actual oxygen transfer capabilities of the system, thus increasing the overall oxidation capability of the system by an additional 55%.

Acknowledgements

We thank Southern Alleghenies Conservancy, the PA Dept of Environmental Protection Resource Recovery Consortium, the Fraunhofer Center for Energy and the Environment, and the University of Pittsburgh for financial support, and the F^2 Machine Shop, Tarentum, PA, and PPC Corporation, Pittsburgh, PA, who fabricated the bench-scale orifice spray reactor.

References

Ackman TE, Kleinmann RLP (1984) In-line aeration and treatment of acid mine drainage. USBM RI 8868, 9 pp

APHA, AWWA, WPCF (1998) Standard Methods for the Examination of Water and Wastewater. 20th edit, Washington, DC

Gogate GR, Pandit AB (2000) Engineering Design Methods for Cavitation Reactors II: Hydrodynamic Cavitation. J American Inst Chem Eng 46: 1641 -1649

Hustwit CC, Ackman TE, Erickson PE (1992) The role of oxygen transfer in acid mine drainage (AMD) treatment. Water Env Research 64: 817-823

Klein, D.B. (2005) An Evaluation of Ferrous Iron Oxidation Kinetics in a Multiple Orifice Spray Reactor. MS Thesis, Dept of Civil and Environmental Engineering, Univ of Pittsburgh, 111 pp

Kolbash, RL, Budeit, D (1988) New Lower Cost Method for Treating Acid Mine Drainage: A Case History – Martinka Mine No. 1. Proc, 49th International Water Conf, Engineers Soc of Western Pennsylvania, p 398 – 92

Kumar P, Kumar M, Pandit AB (2000) Experimental quantification of chemical effects of hydrodynamic cavitation. Chem Eng Science 55: 1633 - 1639

Metcalf & Eddy (2003) Wastewater Engineering, Treatment and Reuse. McGraw-Hill, Inc New York, NY, 1819 pp

Shah YT, Pandit AB, Moholkar VS (1999) Cavitation Reaction Engineering. Kluwer Academic/Plenum Publ, New York, NY, 352 pp

Smith, WH, Werner, RH (1984) Barret, Haentjens & Co. Mixing Apparatus. U.S. Patent # 4,474,477

Stumm W, Lee FG (1961) Oxygenation of Ferrous Iron. Ind Eng Chem 53: 143

Stumm W, Morgan J (1996) Aquatic Chemistry Chemical Equilibria and Rates in Natural Waters. John Wiley & Sons, Inc, New York, NY, 1022 pp

Suslick K, Mdleleni M, Ries JT (1997) Chemistry induced by hydrodynamic cavitation. J Am Chem Soc 119: 9303 – 9304

Tseng KT, Collicott SH (2000) Fluidic spray control. ILASS Americas, 16th Annual Conf on Liquid Atomization and Spray Systems, Monterey, CA

Submitted Feb. 1, 2005; accepted Sept. 19, 2005